

Crystallographic and Spectroscopic Characterization of Tetrakis(μ -*N,N'*-diarylformamidinato)dichlorodirhenium(III,III) Compounds

Judith L. Eglin,^{*,[a]} Chun Lin,^[b] Tong Ren,^[b] Laura Smith,^[a] Richard J. Staples,^[c] and David O. Wipf^[a]

Keywords: Metal–metal bonds / Rhenium / Formamidinate / UV/Vis spectroscopy / Electrochemistry

Through a variation in the aryl substituents of the formamidinate ligand, a variety of dirhenium compounds has been synthesized with $[\text{XArNC(H)NArX}]^-$ where Ar is a substituted C_6H_5 or C_6H_4 aryl ring and X is *p*-MeO (**1**), H (**3**), *m*-MeO (**4**), *p*-Cl (**5**), *m*-Cl (**6**), *m*-CF₃ (**7**), *p*-CF₃ (**8**), 3,4-Cl₂ (**9**), and 3,5-Cl₂ (**10a**, **10b**). UV/Vis and NMR spectroscopy and electrochemical data for **1** and **3–10** have been obtained. X-ray crystallographic analysis of $\text{Re}_2\text{Cl}_2(\mu\text{-form})_4$ with four

different diarylformamidinate ligands and one analog with two different interstitial solvents are presented; $\text{Re}_2\text{Cl}_2[(p\text{-MeOC}_6\text{H}_4)\text{NCHN}(p\text{-MeOC}_6\text{H}_4)]_4$ (**1**), $\text{Re}_2\text{Cl}_2[(m\text{-MeOC}_6\text{H}_4)\text{NCHN}(m\text{-MeOC}_6\text{H}_4)]_4 \cdot 2 \text{CH}_2\text{Cl}_2$ (**4**), $\text{Re}_2\text{Cl}_2[(3,4\text{-Cl}_2\text{C}_6\text{H}_3)\text{NCHN}(3,4\text{-Cl}_2\text{C}_6\text{H}_3)]_4 \cdot 2 \text{CH}_2\text{Cl}_2$ (**9**), $\text{Re}_2\text{Cl}_2[(3,5\text{-Cl}_2\text{C}_6\text{H}_3)\text{NCHN}(3,5\text{-Cl}_2\text{C}_6\text{H}_3)]_4 \cdot 4 \text{CH}_2\text{Cl}_2$ (**10a**), and $\text{Re}_2\text{Cl}_2[(3,5\text{-Cl}_2\text{C}_6\text{H}_3)\text{NCHN}(3,5\text{-Cl}_2\text{C}_6\text{H}_3)]_4 \cdot \text{OC}_4\text{H}_8$ (**10b**).

Introduction

Amidine and amidinate ligands are adaptable ligands in the synthesis of dinuclear transition metal compounds that span the periodic table.^[1] Dinuclear transition metal complexes include Ti_2 ,^[2–4] Zr_2 ,^[5] V_2 ,^{[6][7]} Ta_2 ,^[8–10] Cr_2 ,^[11–13] Mo_2 ,^[11,13–18] W_2 ,^[12] Ta_2 ,^[19] Re_2 ,^{[20][21]} Fe_2 ,^[22–25] Ru_2 ,^[26–32] Os_2 ,^[33] Co_2 ,^[25,34–37] Rh_2 ,^[34,38–41] Ni_2 ,^[42–44] Pd_2 ,^{[44][45]} Pt_2 ,^{[46][47]} Cu_2 ,^[48] Ag_2 ,^{[48][49]} In_2 ,^[50] and Sn_2 ,^[51] and the diversity of dinuclear complexes demonstrates the versatility of the ligand to form both metal–metal bonded and non-bonded systems. Recently, the systematic study of the tunability of the electronic and spectroscopic properties of the resultant complexes with variations in the ligand periphery has become a focus area.^[14,15,26–28,43,52,53]

Redox tuning of dinuclear compounds by varying the remote substituents on the aryl ring of diarylformamidinate ligands (form) has been studied in a series of dichromium(II,II),^[52] dimolybdenum(II,II),^{[14][15]} and dinickel(II,II)^[43] complexes. In the previously studied dinickel systems, metal–metal bonding is absent with a long Ni–Ni separation of 2.462(2) Å observed for $\text{Ni}_2[(3,5\text{-Cl}_2\text{C}_6\text{H}_3)\text{NCHN}(3,5\text{-Cl}_2\text{C}_6\text{H}_3)]_4$.^[43] In contrast, the $\text{Cr}_2(\mu\text{-form})_4$ and $\text{Mo}_2(\mu\text{-form})_4$ systems contain metal–metal quadruple bonds, $\sigma^2\pi^4\delta^2$, with much shorter Cr–Cr and Mo–Mo mean bond lengths of 1.911 and 2.096 Å.^{[15][52]} The study is extended to correlate structural, spectroscopic, and electrochemical properties of $\text{Cr}_2^{\text{II,II}}$, $\text{Mo}_2^{\text{II,II}}$, and $\text{Re}_2^{\text{III,III}}$ quadruply-bonded complexes with the inclusion of

the $\text{Re}_2\text{Cl}_2(\mu\text{-form})_4$ series.^[20,21,52] The addition of the $\text{Re}_2\text{Cl}_2(\mu\text{-form})_4$ complexes allows the comparison of compounds with axially coordinated chlorides and the relativistic effects associated with 5d orbitals to the $\text{Cr}_2(\mu\text{-form})_4$ and $\text{Mo}_2(\mu\text{-form})_4$ systems previously studied.^[20,21,52] A series of dirhenium compounds of the general type $\text{Re}_2\text{Cl}_2(\mu\text{-form})_4$ has been synthesized with the ligand $[\text{XArNC(H)NArX}]^-$, where Ar is a substituted C_6H_5 or C_6H_4 ring and X is *p*-MeO (**1**), H (**3**), *m*-MeO (**4**), *p*-Cl (**5**), *m*-Cl (**6**), *m*-CF₃ (**7**), *p*-CF₃ (**8**), 3,4-Cl₂ (**9**), and 3,5-Cl₂ (**10a**, **10b**). UV/Vis, ¹H-NMR, and ¹³C-NMR spectroscopy are reported for the series in addition to the structural characterization of **1**, **4**, **9**, and **10a**, **b**. A linear free energy relationship is determined from electrochemical studies of the $\text{Re}_2\text{Cl}_2(\mu\text{-form})_4$ complexes by varying the remote substituents on the aryl ring of the diarylformamidinate ligands.

Results and Discussion

Synthesis

Synthesis of compounds **1** and **3–10** with the general formula $\text{Re}_2\text{Cl}_2(\mu\text{-form})_4$ proceeds as previously described.^[21] Molten reactions of $\text{Re}_2\text{Cl}_2(\mu\text{-O}_2\text{CCH}_3)_4$ with the respective substituted diarylformamidinate ligands were performed using a minimum four fold excess of the ligand (Hform) at reaction temperatures between 150° to 180° for 1.5 to 18 hours. Reaction times are dependent on the melting point of the diarylformamidinate ligands. A short reaction time results in incomplete ligand substitution and an elevated reaction temperature leads to thermal decomposition of the diarylformamidinate ligand.

Molecular Structures

¹H-NMR spectra were recorded for compounds **1** and **3–10** to confirm the expected diamagnetic ground state for

^[a] Department of Chemistry, Box 9573, Mississippi State University, Mississippi State, MS 39762, USA

^[b] Department of Chemistry, Florida Institute of Technology, Melbourne, FL 32901, USA

^[c] Department of Chemistry and Chemical Biology, Harvard University, Cambridge, MA 02138, USA

all of the compounds, $\sigma^2\pi^4\delta^2$. The simplicity of the ^1H -NMR spectra reflects the high symmetry of the $\text{Re}_2\text{Cl}_2(\mu\text{-form})_4$ complexes and confirms both the bulk purity of the compounds and the general structure of the compounds where X-ray crystallographic data were not obtained.^[21] The downfield shift of the singlet for the methine proton ($-\text{NCHN}-$) is a distinct feature in the ^1H -NMR spectra of the $\text{Re}_2\text{Cl}_2(\mu\text{-form})_4$ series and ^1H -NMR data combined with structural data for **1**, **4**, **9**, and **10a, b** allowed the calculation of the value of the diamagnetic anisotropy of the Re-Re bond. ^{13}C -NMR spectra were recorded for all of the compounds except **3** and **9** where the solubility of the compounds in CH_2Cl_2 is limited. As a result of poor solubility in most common solvents, the ^{13}C -NMR spectrum of **1** and **4** do not have $-\text{OCH}_3$ peaks tabulated due to an overlap of the methoxy carbon peak of the compound with the carbon peak of the CH_2Cl_2 solvent which dominates the spectrum.

Crystal structures have been determined for $\text{Re}_2\text{Cl}_2[(p\text{-MeOC}_6\text{H}_4)\text{NCHN}(p\text{-MeOC}_6\text{H}_4)]_4$ (**1**), $\text{Re}_2\text{Cl}_2[(m\text{-MeOC}_6\text{H}_4)\text{NCHN}(m\text{-MeOC}_6\text{H}_4)]_4 \cdot 2 \text{CH}_2\text{Cl}_2$ (**4**), $\text{Re}_2\text{Cl}_2[(3,4\text{-Cl}_2\text{C}_6\text{H}_3)\text{NCHN}(3,4\text{-Cl}_2\text{C}_6\text{H}_3)]_4 \cdot 2 \text{CH}_2\text{Cl}_2$ (**9**), $\text{Re}_2\text{Cl}_2[(3,5\text{-Cl}_2\text{C}_6\text{H}_3)\text{NCHN}(3,5\text{-Cl}_2\text{C}_6\text{H}_3)]_4 \cdot 4 \text{CH}_2\text{Cl}_2$ (**10a**), and $\text{Re}_2\text{Cl}_2[(3,5\text{-Cl}_2\text{C}_6\text{H}_3)\text{NCHN}(3,5\text{-Cl}_2\text{C}_6\text{H}_3)]_4 \cdot \text{OC}_4\text{H}_8$ (**10b**), with **10a** and **10b** containing the same diarylformamidinate ligand with two different interstitial solvent molecules. Structures of **1**, **4**, **9**, and **10a, b** are shown in Figures 1–5, and reflect the D_4 geometry adopted by the dirhenium core ($\text{Re}_2\text{N}_8\text{Cl}_2$) in the molecules.

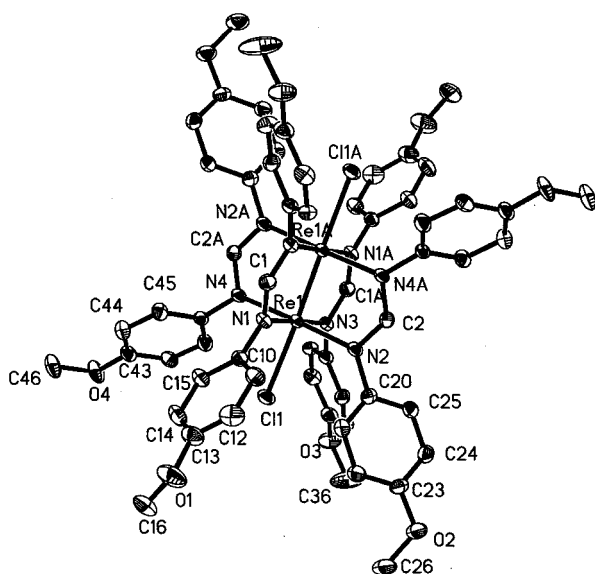


Figure 1. The ORTEP plot of compound **1**; hydrogen atoms are omitted for clarity

A comparison of the Hammett constant of the ligand versus the Re-Re and Re-Cl bond lengths of **1**, **4**, **9**, and **10a, b** and $\text{Re}_2\text{Cl}_2[(p\text{-tolylC}_6\text{H}_4)\text{NCHN}(p\text{-tolylC}_6\text{H}_4)]_4$ (**2**)^[21] indicates the electron donating or withdrawing ability of the ligand has no substantial influence on the bond lengths or angles in the structure (Table 1). The most significant deviation in the Re-Re bond lengths within the series occurs as a result of a change in the interstitial sol-

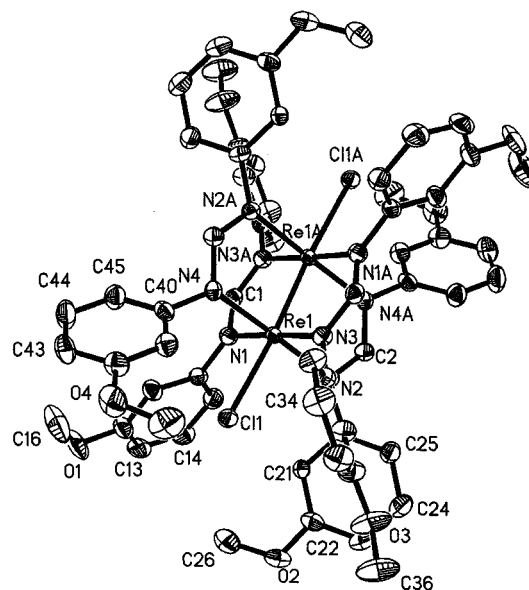


Figure 2. The ORTEP plot of compound **4**; hydrogen atoms and the dichloromethane solvent molecules are omitted for clarity

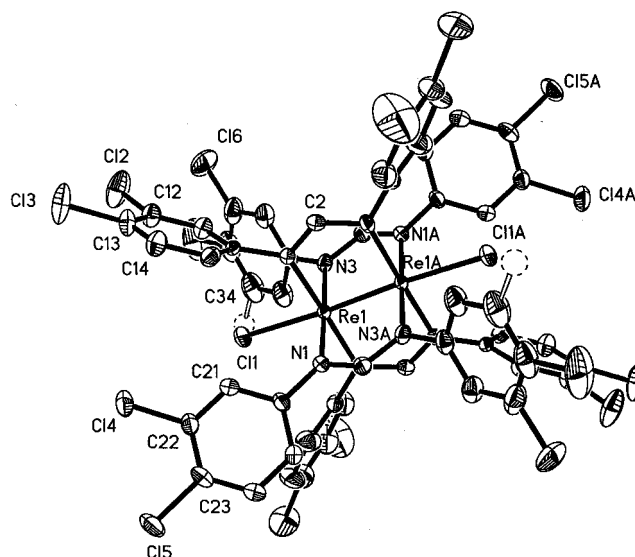


Figure 3. The ORTEP plot of compound **9**; hydrogen atoms and the dichloromethane solvent molecules are omitted for clarity

vent, as in the case of $\text{Re}_2\text{Cl}_2[(3,5\text{-Cl}_2\text{C}_6\text{H}_3)\text{NCHN}(3,5\text{-Cl}_2\text{C}_6\text{H}_3)]_4$ with Re-Re bond lengths of 2.2734(3) Å ($4 \text{CH}_2\text{Cl}_2$) and 2.2840(5) Å (OC_4H_8). More dramatic changes in the structure of the amidinate ligand result in more significant changes in the observed bond lengths and angles.^[20] For $\text{Re}_2\text{Cl}_2[(\text{CH}_3\text{N})_2\text{CPh}]_4$ with the N,N' -dimethylbenzamidinate ligand and Re-Re and Re-Cl bond lengths of 2.208(2) and 2.654(6) Å, the Re-Cl bond length is significantly elongated in comparison to the diarylformamidinate derivatives due to steric repulsions.^[20] As observed in the $\text{Re}_2\text{Cl}_2(\mu\text{-form})_4$ series, only minor variations in the core bond lengths with changes in the substituents on the diarylformamidinate ligands occur for $\text{Cr}_2(\mu\text{-form})_4$, $\text{Mo}_2(\mu\text{-form})_4$, and $\text{Ni}_2(\mu\text{-form})_4$ complexes.^[14,15,43,52,54–57]

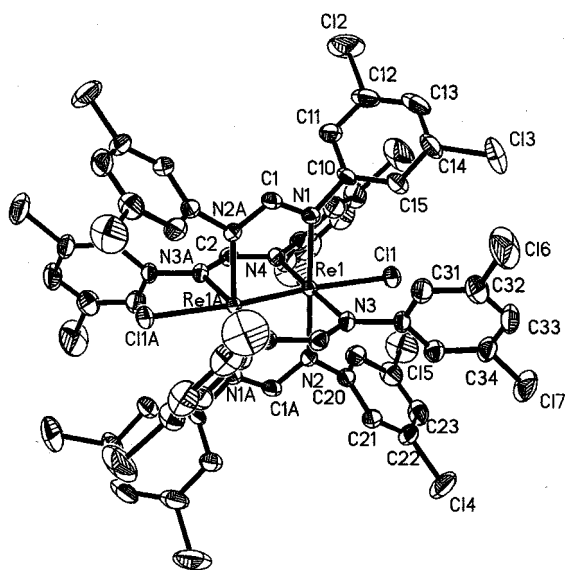


Figure 4. The ORTEP plot of compound **10a**; hydrogen atoms and the dichloromethane solvent molecules are omitted for clarity

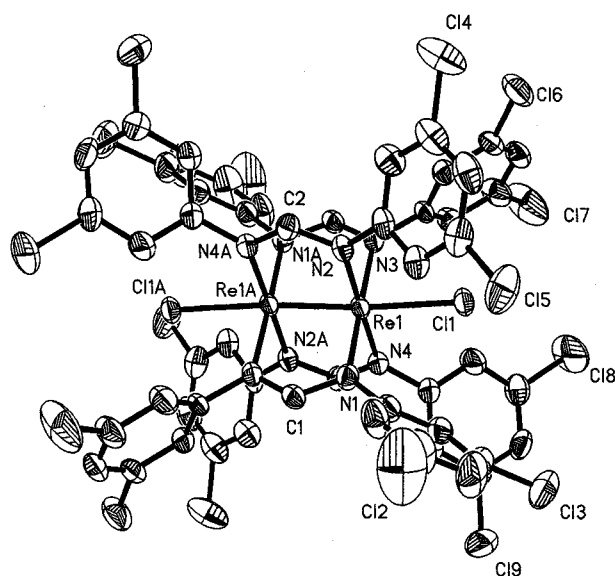


Figure 5. The ORTEP plot of compound **10b**; hydrogen atoms and the THF solvent molecule are omitted for clarity

In order to include relativistic effects of the 5d orbitals and the influence of axially coordinated chlorides in the comparison of the metal–metal bond lengths, the “formal shortness ratio” (FSR) is used to minimize changes in the bond length due to the size of the metal atoms. To determine the FSR for a bond A–B, Equation 1 is applied where D_{A-B} is the distance between the atoms, R_1^A is the radius of atom A, and R_1^B is the radius of atom B.^[58] The FSR has been calculated for the $\text{Cr}_2(\mu\text{-form})_4$ [0.806], $\text{Mo}_2(\mu\text{-form})_4$ [0.809], and $\text{W}_2(\mu\text{-form})_4$ [0.839] complexes using the average M–M bond lengths for the diarylformamidinate analogs.^[12,43,52,59] Using the average Re–Re bond length (2.2776 Å) in the $\text{Re}_2\text{Cl}_2(\mu\text{-form})_4$ series and a radius of 1.283 Å for the Re atom,^{[21][60]} the FSR of the Re–Re bond [0.888] is significantly larger than the FSR for the group 6

Table 1. Selected bond lengths [Å] and angles [°] for **1**, **4**, **9**, and **10a, b**

Compound	1	4	9	10a	10b
Re–Re	2.2777(3)	2.2765(6)	2.2783(4)	2.2734(3)	2.2840(5)
Re–N	2.093(3)	2.089(4)	2.095(4)	2.095(3)	2.081(5)
	2.097(3)	2.096(4)	2.096(4)	2.097(3)	2.095(5)
	2.098(3)	2.104(4)	2.102(4)	2.101(3)	2.104(5)
	2.101(3)	2.115(4)	2.119(4)	2.113(3)	2.104(5)
Re–Cl	2.5212(9)	2.486(1)	2.500(1)	2.4897(9)	2.492(2)
Re–Re–Cl	176.63(2)	175.60(3)	173.55(4)	175.39(3)	174.47(4)
N–Re–N	90.0(1)	89.9(2)	89.4(2)	89.3(1)	89.7(2)
	89.9(1)	88.8(2)	89.6(2)	90.0(1)	90.5(2)
	89.9(1)	89.9(2)	90.6(2)	90.6(1)	89.6(2)
	90.2(1)	91.4(2)	90.4(2)	90.1(1)	90.1(2)
	178.6(1)	178.3(2)	178.6(2)	178.5(1)	178.7(2)
	178.5(1)	178.8(2)	178.7(2)	178.7(1)	178.6(2)
N–Re–Re	91.49(8)	91.0(1)	90.5(1)	91.96(8)	92.7(1)
	91.25(8)	92.1(1)	92.5(1)	91.68(9)	90.6(1)
	89.86(8)	90.1(1)	90.7(1)	89.70(9)	88.5(1)
	90.30(8)	89.1(1)	88.7(1)	89.35(8)	90.6(1)
N–Re–Cl	91.24(8)	89.3(1)	90.0(1)	91.39(9)	92.8(1)
	90.72(8)	92.3(1)	93.9(1)	91.53(9)	89.9(1)
	87.41(8)	89.7(1)	89.1(1)	87.14(9)	86.0(1)
	87.73(8)	86.5(1)	84.8(1)	87.30(9)	88.9(1)
N–C–N	123.5(3)	123.0(5)	122.6(5)	121.8(3)	122.8(6)
	123.4(3)	123.1(5)	122.4(5)	122.1(3)	121.2(6)

$\text{M}_2(\mu\text{-form})_4$ series due to coulombic repulsion between the Re^{III} centers^[21] and larger than the FSR for $[\text{Re}_2\text{Cl}_8]^{2-}$ [0.869] due to the presence of two axial chlorides.^{[58][61]}

$$\text{FSR}_{AB} = D_{A-B}/(R_1^A + R_1^B) \quad (1)$$

Electrochemistry

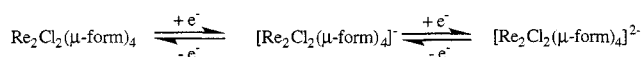
Electrochemical studies of the compounds in the $\text{Re}_2\text{Cl}_2(\mu\text{-form})_4$ series were performed in CH_2Cl_2 under nitrogen. Data were obtained at scan rates of 20, 50, 100, and 200 mV/s to determine the values of the first $[E_{1/2}^1]$ and second $[E_{1/2}^2]$ quasireversible one-electron reduction potentials of compounds **1–4** (Table 2). Prior electrochemical studies of **2**, abbreviated $\text{Re}_2\text{Cl}_2(\mu\text{-DFM})_4$,^[21] were repeated in order to compare electrochemical data performed under the same experimental conditions. As shown in Scheme 1, successive reduction of $\text{Re}_2\text{Cl}_2(\mu\text{-form})_4$ produces $[\text{Re}_2\text{Cl}_2(\mu\text{-form})_4]^-$ and subsequently $[\text{Re}_2\text{Cl}_2(\mu\text{-form})_4]^{2-}$.

Table 2. Hammett constant (σ) of the remote substituents of the formamidinate ligands, $E_{1/2}^1$, and $E_{1/2}^2$ values for electrochemical studies of the $\text{Re}_2\text{Cl}_2(\mu\text{-form})_4$ compounds, **1–4**, with two one-electron quasireversible reductions

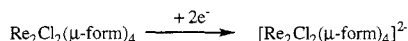
Compound	Hammett constant	$E_{1/2}^1$	$E_{1/2}^2$
1	−0.27	−1.41	−1.68
2	−0.17	−1.39	−1.67
3	0.00	−1.28	−1.55
4	0.12	−1.25	−1.53

A least-squares fit of the $E_{1/2}$ values versus 8σ according to Equation 2 is linear with a slope of ρ , the reactivity constant, period The Hammett constant, σ , is multiplied by eight to account for all of the remote substituents on aryl

Two Successive One-Electron Reductions
for Electron Donating Substituents on the Formamidinate Ligands



Two-Electron Reduction Resulting in Decomposition
for Electron Withdrawing Substituents on the Formamidinate Ligands



Scheme 1

rings of the diarylformamidinate ligands. An anodic shift of the reduction with an increase in the value of the Hammett constants for the diarylformamidinate ligands is observed for **1–4** for both successive one-electron reductions of the dirhenium(III,III) core. At a scan rate of 100 mV/s, the correlation coefficient of the least squares fit of the plot of 8σ versus the $E_{1/2}^1$ value for $\text{Re}_2\text{Cl}_2(\mu\text{-form})_4$ series is 0.990 with ρ equal to 61 mV. When the average of the quasireversible reduction potentials observed at all scan rates is used, as shown in Figure 6, the correlation coefficient of the least squares fit to 8σ versus $E_{1/2}^1$ decreases [0.982] with a slight decrease in ρ , 56 mV.

$$\Delta E_{1/2} = E_{1/2}(\text{X}) - E_{1/2}(\text{H}) = \rho 8\sigma_{\text{X}} \quad (2)$$

where X is the substituent on the formamidinate ligand and H is a hydrogen atom

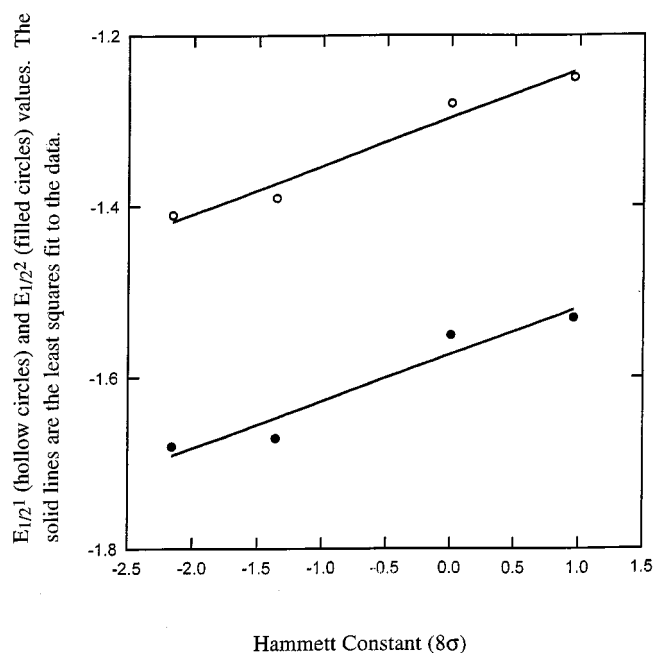


Figure 6. Dependence of $E_{1/2}^1$ (hollow circles) and $E_{1/2}^2$ (filled circles) values using the average of all scan rates on the Hammett constant (8σ) for the $\text{Re}_2\text{Cl}_2(\mu\text{-form})_4$ series. The circles represent the experimental data and the solid lines are the least squares fit to the data

For the $E_{1/2}^2$ values, correlation coefficients of the linear least squares fit of the data of 0.968 and 0.966 with ρ values

of 51 mV (100 mV/s) and 55 mV (all scan rates, as shown in Figure 6) are observed. The $E_{1/2}^1$ values for the $\text{Re}_2\text{Cl}_2(\mu\text{-form})_4$ series varied over 160 mV and $E_{1/2}^2$ values over 150 mV for **1–4** (Table 2) and reflect the ability to use remote substituents to fine tune the electrochemical properties at a dinuclear core.^[15,43,52,62] A similar trend is observed for $\text{Re}_2\text{Cl}_2(\mu\text{-O}_2\text{CR})_4$ complexes with alkyl carboxylates. Plots of $E_{1/2}$ values versus the Taft σ^* parameter, an indicator of the electron donating or withdrawing ability of the carboxylates, are linear.^[62] The anodic shift of the oxidation with increasing values of the Hammett constant of the form ligand is also observed in the $\text{Ni}_2(\mu\text{-form})_4$,^[43] $\text{Cr}_2(\mu\text{-form})_4$,^[52] and $\text{Mo}_2(\mu\text{-form})_4$ ^[15] series.

Studies of the $\text{M}_2(\text{mhp})_4$ series where M_2 is Cr_2 , CrMo , Mo_2 , MoW , and W_2 and mhp is the 2-oxo-6-methylpyridine ion have demonstrated the first oxidation half potential correlates with the energy of the highest occupied molecular orbital as determined by photoelectron spectroscopy [PES].^[63] For the series $\text{Ni}_2(\mu\text{-form})_4$ [$\rho = 114$ mV],^[43] $\text{Cr}_2(\mu\text{-form})_4$ [$\rho = 52.8$ mV],^[52] $\text{Mo}_2(\mu\text{-form})_4$ [$\rho = 87.2$ mV],^[15] and $\text{Re}_2\text{Cl}_2(\mu\text{-form})_4$ [56 mV ($E_{1/2}^1$), 55 mV ($E_{1/2}^2$)], the magnitude of the value of ρ correlates to the ligand character of the orbital where the loss of the electron (oxidation) or gain of the electron (reduction) occurs. For the $\text{Ni}_2(\mu\text{-form})_4$ series with a large reactivity constant, the HOMO involved in the oxidation is the $6b_1$ orbital with 58% Ni and 42% N character.^[44] A smaller reactivity constant is observed for the oxidation of the $\text{Mo}_2(\mu\text{-form})_4$ series^[15] with a $2b_{2g}$ HOMO orbital with 87% Mo and 4% N character.^[18]

The reactivity constants calculated for the $\text{Re}_2\text{Cl}_2(\mu\text{-form})_4$ complexes **1–4** are lower than either the dinickel or dimolybdenum series and similar for both reductions. Since a reduction is occurring, the orbital of interest in the determination of the value of ρ for both $E_{1/2}^1$ and $E_{1/2}^2$ is the LUMO, $6e_g$, with 91% Re and 1% N character. Very little change in the ligand character of the electrochemically active orbital is observed upon reduction to $\text{Re}_2(\text{HNC}(\text{H})\text{NH})_4$ with 97% Re and 2% N character for the $5e_g$ orbital.^[21] The general trend observed in the $\text{M}_2(\mu\text{-form})_4$ complexes is a dependence of the reactivity constant on the ligand character of the orbital involved in either the reduction (LUMO) or oxidation (HOMO). With an increase in the ligand character of the electrochemically active orbital, the $E_{1/2}$ value is more strongly dependent on changes in the remote substituents of the ligand.

In contrast to the two one-electron reductions observed for **1–4**, studies of compounds **5–10** (Table 3) with more electron-withdrawing substituents on the diarylformamidinate ligands resulted in an irreversible two-electron reduction of the compound, as demonstrated by a ratio of peak currents of 2.48 (a ratio of 2.83 is predicted for compounds **5–10** versus **1–4** based on no change in diffusion coefficients and concentrations^[64]). Two-electron reductions result when the loss of a second electron occurs more easily than the first electron due to an inversion of the reduction potentials^[65] and are the result of a structural change.^[65–69] For example, the electrochemistry of $[\text{Mo}_2\text{Cp}_2(\text{CO})_4]\mu\text{-}$

$\eta^2:\eta^3\text{-HCC-C(R1)(R2)]}^+$ complexes is controlled by the R1 and R2 substituents as a result of changes in the energy of the LUMO orbital.^[66]

To explain the change in the redox behavior of the $\text{Re}_2\text{Cl}_2(\mu\text{-form})_4$ complexes^[57] with more electron-withdrawing substituents, the relative energies of the orbitals involved in the reduction were investigated. Fenske–Hall calculations performed on the $\text{Mo}_2(\mu\text{-form})_4$ series indicate the δ^* orbital (LUMO) with approximately 76% metal character increases in energy by 1.18 eV upon a change in the remote substituent of the formamidinate ligand from 3,5-dichloro to *p*-MeO.^[15] In contrast, the σ^* orbital with approximately 87% metal character increases in energy by only 0.83 eV with the same variation in the remote substituents.^[15] The Fenske–Hall calculations^[15] demonstrate that, with increasing ligand character of a particular orbital, a more significant change in the orbital energy occurs with a change in the ligand substituents.

The orbitals of predominantly metal character for $\text{Re}_2\text{Cl}_2(\mu\text{-DFM})_4$ are, in order of increasing energy, $5a_{1g}$ (σ , -14.22 eV), $5e_u$ (π , -11.225 eV), $2b_{2g}$ (δ , -8.804 eV), $6e_g$ (π^* , LUMO, -7.174 eV), $2b_{1u}$ (δ^* , -6.912 eV), and $6a_{2u}$ (σ^* , -3.295 eV). Only a -0.262 eV difference in energy is predicted between the two lowest unoccupied orbitals (π^* and δ^*) with Re characters of 91% and 59%, respectively.^[21] Based on the trend observed in the previous studies of $\text{Mo}_2(\text{form})_4$,^{[15][21]} the energy of the δ^* orbital decreases more rapidly than the π^* orbital with an increase in the electron-withdrawing ability (σ) of the remote substituent on the aryl group of the formamidinate ligand in $\text{Re}_2\text{Cl}_2(\mu\text{-form})_4$ complexes. The energy difference between the π^* and δ^* orbitals diminishes or even becomes negative with increasing σ , as shown in Figure 7. As a result of the change in the orbital manifold across the series of $\text{Re}_2\text{Cl}_2(\mu\text{-form})_4$ complexes, two quasireversible one-electron reductions occur for the electron donating substituents and an irreversible two-electron reduction occurs for the electron-withdrawing substituents. Although the same general trend in reduction potentials is observed for both the one-electron quasireversible and two-electron irreversible reduction of the $\text{Re}_2\text{Cl}_2(\mu\text{-form})_4$ complexes as shown in Tables 2 and 3, a linear least squares fit of the Hammett constant versus the two-electron irreversible reduction at 100 mV [Table 3] is poor with a correlation coefficient of 0.832 and a ρ value of 44 mV. The electrochemical decomposition product is subsequently oxidized but has not been structurally or spectroscopically characterized.

Electronic Spectra

The electronic spectra of **1** and **3–10** consist of an intense peak between 386 to 418 nm. The transition at 403 nm for $\text{Re}_2\text{Cl}_2[(p\text{-tolylC}_6\text{H}_4)\text{NCHN}(p\text{-tolylC}_6\text{H}_4)]_4$ ^[21] is assigned to the δ to δ^* transition. The intense peak occurring between 386 and 418 nm in the $\text{Re}_2\text{Cl}_2(\mu\text{-form})_4$ series is assigned to the same transition with no correlation between the Hammett constants of the remote substituents and the energy of the δ to δ^* transition observed.^[15,54–57]

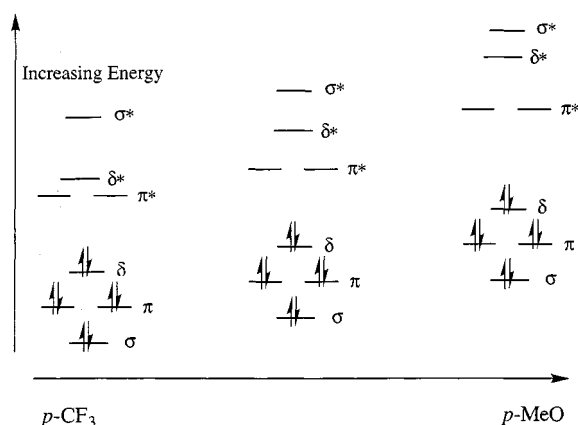


Figure 7. The predicted change in the orbital manifold across the series of $\text{Re}_2\text{Cl}_2(\mu\text{-form})_4$ complexes with changes in the Hammett constant of the remote substituent of the formamidinate ligand

Table 3. Hammett constant (σ) of the remote substituents of the formamidinate ligands and E_{pc} values for electrochemical studies of the $\text{Re}_2\text{Cl}_2(\mu\text{-form})_4$ compounds, **5–10**, with two-electron irreversible reductions

Compound	Hammett constant	E_{pc}
5	0.23	-1.52
6	0.37	-1.53
7	0.43	-1.48
8	0.54	-1.50
9	0.60	-1.36
10a, 10b	0.74	-1.37

Diamagnetic Anisotropy of the Re–Re Bond

An induced field from circulating electrons results in the diamagnetic anisotropy in transition metal complexes containing metal-metal multiple bonds. In the $\text{Re}_2\text{Cl}_2(\mu\text{-form})_4$ series, the methine proton ($-\text{NCHN}-$) of the bridging diarylformamidinate ligand is affected by the induced field caused by the circulating electrons of the Re–Re quadruple bond. As a result, the methine proton is deshielded and a downfield chemical shift is observed. From the chemical shift difference of the methine proton [$\Delta\delta = \delta(-\text{NCHN}-\text{Re}_2) - \delta(-\text{NCHN}-\text{Ni}_2)$]^[43] and structural parameters of these protons (r and θ) extracted from the crystallographic data, the diamagnetic anisotropy for the Re–Re bond is calculated from Equation 3 shown below.^[70]

$$\Delta\delta = \frac{\Delta\chi}{4\pi} \left[\frac{1 - 3 \cos^2 \theta}{3r^3} \right]$$

The $\Delta\chi$ values calculated based on crystallographic and ^1H spectroscopic data for $\text{Re}_2\text{Cl}_2(\mu\text{-form})_4$ with the substituents *p*-MeO, *m*-MeO, 3,5- Cl_2 , and 3,4- Cl_2 are 4034, 3890, 3940, and $4154 \cdot 10^{-36} \text{ m}^3 \text{ molecule}^{-1}$, respectively or $4004 \cdot 10^{-36} \text{ m}^3 \text{ molecule}^{-1}$ on average. Since the chemical shift of the methine proton of $\text{Ni}_2[(3,4\text{-Cl}_2\text{C}_6\text{H}_3)\text{NCHN}(3,4\text{-Cl}_2\text{C}_6\text{H}_3)]_4$ is not available, the chemical shift was estimated ($\delta = 6.185$) based on the average

change in the methine proton chemical shift upon coordination to the Ni_2 core from values of nine reported $\text{Ni}_2(\mu\text{-form})_4$ complexes and the corresponding free ligands.^[43] The values are somewhat smaller than $\Delta\chi$ value of $4430 \cdot 10^{-36} \text{ m}^3 \text{ molecule}^{-1}$ reported previously for $\text{Re}_2\text{Cl}_2(\mu\text{-DFM})_4$.^[12] The correlation of the diamagnetic anisotropy to the Hammett constant of the remote substituents on the diarylformamidinate ligands for the $\text{Re}_2\text{Cl}_2(\mu\text{-form})_4$ series is extremely poor.

Conclusions

With the synthesis of a series of $\text{Re}_2\text{Cl}_2(\mu\text{-form})_4$ compounds incorporating a variety of electron donating and withdrawing remote substituents on the diarylformamidinate ligands, the comparison of structural and spectroscopic properties of $\text{M}_2(\mu\text{-form})_4$ complexes is extended to include dirhenium(III,III) compounds with axially coordinated chlorides. In the metal–metal bonded, $\text{Cr}_2(\mu\text{-form})_4$, $\text{Mo}_2(\mu\text{-form})_4$, and $\text{Re}_2\text{Cl}_2(\mu\text{-form})_4$, and non-bonded systems, $\text{Ni}_2(\mu\text{-form})_4$, which have variations in the Hammett constant of the remote substituents on the diarylformamidinate ligands, no correlation between the metal–metal bond lengths or metal–nitrogen bond lengths and σ is observed.^[14,15,43,52]

The two quasireversible one-electron reductions for **1–4** and the two-electron irreversible reductions observed for **5–10** reflect the ability to tune the reduction potential over a 150 mV range (**1–4**) via the remote substituents on the diarylformamidinate ligand.^[14,15,43,52,66] The reactivity constants of the $\text{Re}_2\text{Cl}_2(\mu\text{-form})_4$ series (**1–4**) are similar in magnitude to the $\text{Cr}_2(\mu\text{-form})_4$ series and significantly smaller than either the $\text{Mo}_2(\mu\text{-form})_4$ or $\text{Ni}_2(\mu\text{-form})_4$ series.^[14,15,43,52] Based on systems where both electrochemical and theoretical data are available, the $E_{1/2}$ value becomes more strongly dependent on changes in the remote substituents on the diarylformamidinate ligand with increasing ligand character of the electrochemically active orbital.^[15,18,21,43,44,52] Studies of a series of $\text{W}_2(\mu\text{-form})_4$ complexes with a variety of substituents on the diarylformamidinate ligands are in progress to determine the effect of the Hammett constant of the ligand substituents on the electrochemical process.

Experimental Section

Starting Materials: The starting materials $[\text{N}(n\text{-Bu})_4]_2[\text{Re}_2\text{Cl}_8]$,^[71] $\text{Re}_2(\mu\text{-O}_2\text{CCH}_3)_4\text{Cl}_2$,^[72] and **2**^[21] were synthesized by the standard literature methods. All the diarylformamidinate ligands were synthesized according to literature methods, washed under an argon atmosphere with freshly distilled hexanes, and transferred to the dry-box.^{[15][73]} The solvents ethanol (EtOH), methanol (MeOH), CH_2Cl_2 , ethyl acetate, and hexanes for the synthesis of the $\text{Re}_2\text{Cl}_2(\mu\text{-form})_4$ complexes were used as received without distillation.

Preparation of the Complexes: $\text{Re}_2\text{Cl}_2[(p\text{-MeOC}_6\text{H}_4)\text{NCHN}(p\text{-MeOC}_6\text{H}_4)]_4$ (**1**). $\text{Re}_2\text{Cl}_2(\mu\text{-O}_2\text{CCH}_3)_4$ (0.090 g, 0.13 mmol) was heated at 140°C with $(p\text{-MeOC}_6\text{H}_4)\text{NHCHN}(p\text{-MeOC}_6\text{H}_4)$ (3 g,

11.7 mmol) under argon for 5 hours. EtOH (40 mL) was added to the molten reaction mixture while hot, and the mixture was vigorously stirred for 1 hour. The orange-yellow solid was collected by filtration and dried under dynamic vacuum. $^1\text{H-NMR}$ spectroscopy revealed the presence of free ligand, and the crude product was further purified by chromatography. Yield: 0.093 g (48.8%). – $^1\text{H NMR}$: δ = 8.30 (s, 4 H), 6.66 (m, 32 H), 3.75 (s, 24 H). – $^{13}\text{C NMR}$ δ : 171.1 (s), 158.1 (s), 145.6 (s), 129.2 (s), 127.7 (s), 113.2 (s), 111.8 (s). – UV/Vis: λ_{max} (nm) = 278, 418.

$\text{Re}_2\text{Cl}_2[(\text{C}_6\text{H}_5)\text{NCHN}(\text{C}_6\text{H}_5)]_4$ (3**):** $\text{Re}_2\text{Cl}_2(\mu\text{-O}_2\text{CCH}_3)_4$ (0.110 mg, 0.16 mmol) was heated at 150°C with $(\text{C}_6\text{H}_5)\text{NHCHN}(\text{C}_6\text{H}_5)$ (2.94 g, 15.0 mmol) under argon for 8 hours. Upon completion of the reaction, the product was extracted with hot ethanol (80 mL), but a clean separation was not achieved. The filtrate and solid were combined and dried on a rotovap. Ethyl acetate (50 mL) was added and the mixture was heated to reflux and the resultant mixture was cold filtered to remove the bulk of the free ligand. The crude product was suspended in 6 mL of CH_2Cl_2 and heated to reflux. Following addition of 30 mL of ethyl acetate and an additional reflux period of 10 minutes, vigorous stirring of the reaction mixture during cooling to room temperature yielded golden flakes of **3**. The solid product was collected by filtration and dried under dynamic vacuum. Yield: 0.142 g (72.5%). – $^1\text{H NMR}$: δ = 8.40 (s, 4 H), 7.13 (d, 16 H, 3J = 1.6 Hz), 7.11 (d, 8 H), 6.76 (dd, 16 H). – $^{13}\text{C NMR}$: δ = 152.2 (s), 128.4 (s), 127.0 (s). – UV/Vis: λ_{max} (nm) = 278, 396.

$\text{Re}_2\text{Cl}_2[(m\text{-MeOC}_6\text{H}_4)\text{NCHN}(m\text{-MeOC}_6\text{H}_4)]_4$ (4**):** $\text{Re}_2\text{Cl}_2(\mu\text{-O}_2\text{CCH}_3)_4$ (0.110 g, 0.16 mmol) was heated at 140°C with $(m\text{-MeOC}_6\text{H}_4)\text{NHCHN}(m\text{-MeOC}_6\text{H}_4)$ (3 g, 11.7 mmol) under argon overnight. Ethyl acetate (35 mL) was added to the molten reaction mixture and the solution refluxed for an hour. The orange-yellow solid was collected by filtration and dried under vacuum. Since TLC indicated incomplete purification, another 35 mL of ethyl acetate was added to the crude product and the mixture refluxed. The purified solid product was collected by filtration and dried under dynamic vacuum. Yield: 0.210 g (89.6%). – $^1\text{H NMR}$: δ = 8.40 (s, 4 H), 7.12 (t, 8 H, 3J = 8.0 Hz), 6.66 (dd, 8 H, 3J = 8.3 Hz, 4J = 1.9 Hz), 6.60 (d, 8 H, 3J = 7.6 Hz), 6.34 (s, 8 H), 3.29 (s, 24 H). – $^{13}\text{C NMR}$: δ = 171.3 (s), 169.9 (s), 158.7 (s), 153.5 (s), 128.9 (s), 127.5 (s), 119.7 (s), 118.2 (s), 114.5 (s), 113.1 (s). – UV/Vis: λ_{max} (nm) = 286, 400.

$\text{Re}_2\text{Cl}_2[(p\text{-ClC}_6\text{H}_4)\text{NCHN}(p\text{-ClC}_6\text{H}_4)]_4$ (5**):** $\text{Re}_2\text{Cl}_2(\mu\text{-O}_2\text{CCH}_3)_4$ (0.17 g, 0.25 mmol) was heated at 180°C with $(p\text{-ClC}_6\text{H}_4)\text{NHCHN}(p\text{-ClC}_6\text{H}_4)$ (2.12 g, 8.0 mmol) under argon for 3 hours. The solid product was dissolved in CH_2Cl_2 and precipitated from solution with EtOH. The orange solid was collected by filtration and dried under dynamic vacuum. Yield: 0.262 g (69.9%). – $^1\text{H NMR}$: δ = 8.32 (s, 4 H), 7.14 (d, 16 H, 3J = 8.6 Hz), 6.63 (d, 16 H, 3J = 8.7 Hz). – $^{13}\text{C NMR}$: δ = 171.3 (s), 150.1 (s), 132.6 (s), 129.3 (s), 128.6 (s), 128.0 (s), 127.2 (s). – UV/Vis: λ_{max} (nm) = 274, 398.

$\text{Re}_2\text{Cl}_2[(m\text{-ClC}_6\text{H}_4)\text{NCHN}(m\text{-ClC}_6\text{H}_4)]_4$ (6**):** $\text{Re}_2\text{Cl}_2(\mu\text{-O}_2\text{CCH}_3)_4$ (0.11 g, 0.16 mmol) was heated at 180°C with $(m\text{-ClC}_6\text{H}_4)\text{NHCHN}(m\text{-ClC}_6\text{H}_4)$ (2.12 g, 8.0 mmol) under argon for 3 hours. Ethyl acetate (15 mL) was added while the molten reaction mixture was still hot. The crude solid product was collected by filtration. The residual free ligand was removed by redissolving the crude product in CH_2Cl_2 and precipitating **6** with hexanes. The orange-yellow solid was collected by filtration and dried under dynamic vacuum. Yield: 0.130 g (54.2%). – $^1\text{H NMR}$: δ = 8.48 (s, 4 H), 7.12–7.21 (m, 16 H), 6.74 (d, 8 H, 4J = 1.9 Hz), 6.73 (s, 8 H). – $^{13}\text{C NMR}$: δ = 171.7 (s), 170.1 (s), 152.5 (s), 133.2 (s), 129.6 (s),

128.6 (s), 128.2 (s), 127.7 (s), 127.3 (s), 126.3 (s), 126.1 (s), 124.7 (s). – UV/Vis: λ_{\max} (nm) = 278, 390.

Re₂Cl₂[(*m*-CF₃C₆H₄)NCHN(*m*-CF₃C₆H₄)]₄ (7): Re₂Cl₂(μ -O₂CCH₃)₄ (0.17 g, 0.25 mmol) was heated at 156 °C with (*m*-CF₃C₆H₄)NHCHN(*m*-CF₃C₆H₄) (3.1 g, 9.3 mmol) for 15 hours. EtOH (40 mL) was added to the reaction mixture while hot. The mixture stirred vigorously for 1 hour. The solid was collected by filtration, washed with 20 mL of EtOH and 10 mL of hexanes, and dried under vacuum. Yield: 0.39 g (88%). – ¹H NMR: δ = 8.57 (s, 4 H), 7.46 (d, 8 H, ³*J* = 7.6 Hz), 7.36 (t, 8 H, ³*J* = 7.9 Hz), 7.08 (d, 8 H, ³*J* = 7.4 Hz), 6.85 (s, 8 H). – ¹³C NMR δ : 171.3 (s), 151.45 (s), 130.12 (s), 128.77 (s), 124.83 (s), 123.93 (s). – UV/Vis: λ_{\max} (nm) = 294, 386.

Re₂Cl₂[(*p*-CF₃C₆H₄)NCHN(*p*-CF₃C₆H₄)]₄ (8): Re₂Cl₂(μ -O₂CCH₃)₄ (0.20 g, 0.30 mmol) was heated at 170 °C with (*p*-CF₃C₆H₄)NHCHN(*p*-CF₃C₆H₄) (2.0 g, 6.0 mmol) for 1.5 hours. After cooling, acetone (20 mL) was added to the reaction mixture and the red-orange supernatant solution transferred from the unchanged ligand. Slow evaporation of the acetone resulted in red-orange crystals. The crystals were washed with 10 mL of hexanes, and dried under vacuum. Yield: 0.305 g (57.5%). – ¹H NMR: δ = 8.47 (s, 4 H), 7.45 (d, 16 H, ³*J* = 3.9 Hz), 6.81 (d, 16 H, ³*J* = 3.9 Hz). – ¹³C NMR: δ = 171.22 (s), 154.38 (s), 129.44 (q, ¹*J*_{C–F} = 33.8 Hz), 127.94 (d, ²*J*_{C–F} = 14.1 Hz), 126.68 (s), 125.51 (s), 122.91 (s), 120.21 (s). – UV/Vis: λ_{\max} (nm) = 386.

Re₂Cl₂[(3,4-Cl₂C₆H₃)NCHN(3,4-Cl₂C₆H₃)]₄ (9): Re₂Cl₂(μ -O₂CCH₃)₄ (0.100 g, 0.15 mmol) was heated at 170 °C with (3,4-Cl₂C₆H₃)NHCHN(3,4-Cl₂C₆H₃) (2.0 g, 6.0 mmol) under dynamic vacuum for 7 hours. Ethanol (30 mL) was added to the orange-brown solid while the reaction mixture was warm. After stirring the solution overnight to dissolve excess ligand, the solution was

filtered and the yellow-orange solid collected on the frit. The purified solid product was dried under dynamic vacuum. Yield: 0.132 g (49.6%). – ¹H NMR: δ = 8.398 (s, 4 H), 7.244 (d, 4 H, ³*J* = 8.5 Hz), 6.699 (d, 4 H, ⁴*J* = 2.4 Hz), 6.603 (dd, 4 H, ³*J* = 8.5 Hz, ⁴*J* = 2.4 Hz). – UV/Vis: λ_{\max} (nm) = 282, 398.

Re₂Cl₂[(3,5-Cl₂C₆H₃)NCHN(3,5-Cl₂C₆H₃)]₄ (10a, 10b): Re₂Cl₂(μ -O₂CCH₃)₄ (0.550 g, 0.81 mmol) was heated at 170 °C with (3,5-Cl₂C₆H₃)NHCHN(3,5-Cl₂C₆H₃) (2.0 g, 6.0 mmol) under dynamic vacuum for 7 hours. The orange-brown solid was loaded on a column of chromatographic Silica Gel of 200 to 425 mesh and eluted with CH₂Cl₂. The yellow solution was collected and dried under dynamic vacuum. The addition of ethanol dissolves the excess ligand and the yellow-orange product was collected by filtration of the ethanol suspension. The purified solid product was dried under dynamic vacuum. Yield: 0.302 g (21.0%). – ¹H NMR: δ = 8.50 (s, 4 H), 7.20 (s, 8 H), 6.6 (d, H, ⁴*J* = 1.8 Hz). – ¹³C NMR: δ = 171.3 (s), 152.3 (s), 134.4 (s), 127.4 (s), 125.9 (s). – UV/Vis: λ_{\max} (nm) = 278, 314, 388.

Physical Measurements: The spectroscopy, UV/Vis and ¹³C-NMR, was performed using CH₂Cl₂ dried over P₂O₅ and freshly distilled under argon prior to use. ¹H-NMR spectra were recorded on either a Bruker AMX-360 NMR spectrometer or a General Electric Omega 400 MHz NMR spectrometer with chemical shifts (δ) referenced to the residual CHCl₃ (δ = 7.27) in the CDCl₃ solvent. ¹³C-NMR spectra were recorded on a General Electric Omega 400 MHz NMR spectrometer with a 10 mm broad band probe with chemical shifts (δ) referenced to CH₂Cl₂ (δ = 54.2). 10-mm NMR tubes for ¹³C-NMR spectra were prepared by dissolving the respective Re₂Cl₂(μ -form)₄ complexes in CH₂Cl₂ with a 4 mm NMR insert of either CDCl₃ or CD₃CD₂OD to lock. ¹³C-NMR spectra required 4 to 24 hours of data collection to obtain reasonable signal

Table 4. Crystallographic data for **1**, **4**, **9**, and **10a, b**

	1	4	9	10a	10 b
Empirical formula	C ₆₀ H ₆₀ Cl ₂ N ₈ O ₈ Re ₂	C ₆₁ H ₇₀ Cl ₄ N ₈ O ₈ Re ₂	C ₅₄ H ₃₁ Cl ₂₂ N ₈ Re ₂	C ₅₆ H ₃₆ Cl ₂₆ N ₈ Re ₂	C ₅₂ H ₂₈ Cl ₁₈ N ₈ ORe ₂
Formula mass	1464.46	1557.45	1944.17	2115.03	1791.32
temp [K]	213(2)	213(2)	213(2)	213(2)	213(2)
wavelength [Å]	0.71073	0.71073	0.71073	0.71073	0.71073
crystal system	monoclinic	monoclinic	orthorhombic	monoclinic	monoclinic
space group	<i>P</i> 2(1)/ <i>n</i> , [#14]	<i>P</i> 2(1)/ <i>c</i> , [#14]	<i>P</i> bca, [#61]	<i>P</i> 2(1)/ <i>n</i> , [#14]	<i>P</i> 2(1)/ <i>n</i> , [#14]
<i>a</i> [Å]	14.822(3)	11.145(3)	21.2457(3)	12.4590(2)	11.2331(2)
<i>b</i> [Å]	12.776(2)	19.654(4)	14.3471(2)	19.7205(3)	17.1592(1)
<i>c</i> [Å]	15.263(2)	14.310(3)	22.0263(1)	16.3497(1)	18.4167(3)
β [deg]	91.452(9)	92.19(1)		110.560(1)	94.731(1)
<i>V</i> [Å ³]	2889.3(8)	3132(1)	6713.9(1)	3761.21(9)	3537.74(9)
<i>Z</i>	2	2	4	2	2
<i>d</i> _{calc} [Mg/m ³]	1.683	1.651	1.923	1.868	1.682
absorption coefficient [mm ^{−1}]	4.340	4.091	4.523	4.182	4.139
crystal size [mm]	0.15 × 0.2 × 0.2	0.25 × 0.25 × 0.25	0.05 × 0.05 × 0.05	0.25 × 0.20 × 0.15	0.10 × 0.10 × 0.10
theta range for data collection [deg]	1.89 to 27.70	1.76 to 28.32	1.85 to 25.00	1.68 to 28.28	1.62 to 24.69
index ranges	−18 ≤ <i>h</i> ≤ 19, −13 ≤ <i>k</i> ≤ 16, −13 ≤ <i>l</i> ≤ 18	−13 ≤ <i>h</i> ≤ 14, −24 ≤ <i>k</i> ≤ 17, −13 ≤ <i>l</i> ≤ 18	−25 ≤ <i>h</i> ≤ 15, −17 ≤ <i>k</i> ≤ 17, −25 ≤ <i>l</i> ≤ 25	−15 ≤ <i>h</i> ≤ 16, −26 ≤ <i>k</i> ≤ 26, −14 ≤ <i>l</i> ≤ 21	−13 ≤ <i>h</i> ≤ 12, −11 ≤ <i>k</i> ≤ 20, −18 ≤ <i>l</i> ≤ 21
reflections collected	11983	15944	27192	22199	17925
independent reflections	5891 [<i>R</i> (int) = 0.0229]	6775 [<i>R</i> (int) = 0.0282]	5800 [<i>R</i> (int) = 0.0416]	9095 [<i>R</i> (int) = 0.0308]	5996 [<i>R</i> (int) = 0.0425]
refinement method	full-matrix least-squares on <i>F</i> ²	full-matrix least-squares on <i>F</i> ²	full-matrix least-squares on <i>F</i> ²	full-matrix least-squares on <i>F</i> ²	full-matrix least-squares on <i>F</i> ²
data/restraints/parameters	5891 / 0 / 362	6775/3/388	5800/0/398	9095/0 /415	5996/0/406
<i>R</i> ^[a] [<i>I</i> > 2σ(<i>I</i>)]	0.0264	0.0393	0.0322	0.0325	0.0550
<i>R</i> _w ^[b] [<i>I</i> > 2σ(<i>I</i>)]	0.0593	0.1008	0.0733	0.0706	0.0778

^[a] $R = \sum ||F_o| - |F_c|| / \sum |F_o|$. – ^[b] $wR = \{ \sum [w(F_o^2 - F_c^2)^2] / \sum [w(F_o^2)] \}^{1/2}$.

to noise levels. Data could not be obtained for **3** or **9** due to poor solubility of the compounds in CH_2Cl_2 . The UV/Vis spectra were recorded on a Hewlett Packard model 8452 diode array spectrophotometer from 250 to 820 nm. Cyclic voltammetry measurements of compounds **1–10** were performed using a Solartron SI 1287 Electrochemical Interface in 0.1 M (*n*Bu₄N)PF₆ electrolyte and 0.6 mM $\text{Re}_2\text{Cl}_2(\mu\text{-form})_4$ solutions with a 1.6-mm diameter Pt disk working electrode and a Ag wire quasi-reference electrode. The CH_2Cl_2 solutions of the respective complexes were purged for 20 minutes with nitrogen before data were recorded. The nitrogen was presaturated with CH_2Cl_2 to minimize solution evaporation. All electrode potentials are reported versus the ferrocene/ferrocenium $E_{1/2}$ value [0 V].

X-ray Crystallographic Study:^[74] Crystals of **1**, **4**, **9**, and **10a**, **b** were grown by slow diffusion of CH_2Cl_2 (**1**, **4**, **9**, and **10a**) or THF (**10b**) solutions of the respective compounds with hexanes. Data were collected for **1**, **4**, **9**, and **10a**, **b** using a Siemens SMART CCD based diffractometer equipped with a LT-2 low-temperature apparatus operating at 213 K. Suitable crystals were mounted on a glass fiber using grease. Data were measured using omega scans of 0.3° per frame for 30 seconds such that a hemisphere was collected. A total of 1271 frames were collected with a final resolution of 0.75 Å (**1**, **4**, and **10a**) and 0.85 Å (**9** and **10b**). The first 50 frames were recollected at the end of data collection for each of the crystals to monitor for decay, but no decomposition during data collection was observed. Cell parameters for **1**, **4**, **9**, and **10a**, **b** were retrieved using SMART^[75] software and refined using SAINT on all observed reflections. Data reductions were performed using SAINT^[76] software which corrects for decay and Lorentz and polarization effects. Absorption corrections were applied using SADABS^[77] supplied by George Sheldrick. The structures were solved by direct methods using the SHELXL-90^[78] program and refined by least squares method on F^2 , SHELXL-93,^[79] incorporated in SHELXTL PC V 5.03.^[80] All non-hydrogen atoms are refined anisotropically. The positions of the hydrogen atoms were determined by difference Fourier methods and refined in **9** and **10a** and were calculated geometrically and refined as a riding model for **1**, **4**, and **10b**. One of the ligands in **9** showed a disorder of the ring to result in a disorder of two of the chloride positions with an occupancy of 50% each. Although the dichloromethane solvent molecules of **4** could not be modeled successfully as disordered, the remaining electron density in the structure resides within the solvent molecule. Selected bond lengths and angles for **1**, **4**, **9**, and **10a**, **b** are listed in Table 1 and pertinent crystallographic parameters are summarized in Table 4.

Acknowledgments

J. L. E. and L. S. would like to acknowledge the support of the National Science Foundation EPSCoR program (Grant # EHR 9108767) and the ARI Program (Grant # CHE-92-14521). T. R. would like to acknowledge the partial support from the Petroleum Research Fund/ACS.

- [1] J. Barker, M. Kilner, *Coord. Chem. Rev.* **1994**, *133*, 219–300.
- [2] P. J. Stewart, A. J. Blake, P. Mountford, *Inorg. Chem.* **1997**, *36*, 3616–3622.
- [3] J. R. Hagadorn, J. Arnold, *Inorg. Chem.* **1997**, *36*, 2928–2929.
- [4] S. Hao, K. Feghali, S. Gambarotta, *Inorg. Chem.* **1997**, *36*, 1745–1748.
- [5] A. Horton, J. deWith, *Organometallics* **1997**, *16*, 5424–5436.
- [6] F. A. Cotton, L. M. Daniels, C. A. Murillo, *Inorg. Chem.* **1993**, *32*, 2881–2885.

- [7] F. A. Cotton, R. Poli, *Inorg. Chim. Acta* **1988**, *141*, 91–98.
- [8] F. A. Cotton, L. M. Daniels, C. A. Murillo, X. Wang, *J. Am. Chem. Soc.* **1996**, *118*, 4830–4833.
- [9] F. A. Cotton, L. M. Daniels, J. H. Matonic, X. Wang, C. A. Murillo, *Polyhedron* **1997**, *16*, 1177–1191.
- [10] F. A. Cotton, L. M. Daniels, C. A. Murillo, X. Wang, *Inorg. Chem.* **1997**, *36*, 896–901.
- [11] F. A. Cotton, D. J. Maloney, J. Su, *Inorg. Chim. Acta* **1995**, *236*, 21–29.
- [12] F. A. Cotton, T. Ren, *J. Am. Chem. Soc.* **1992**, *114*, 2237–2242.
- [13] W. H. DeRoode, K. Vrieze, *J. Organomet. Chem.* **1977**, *135*, 183–193.
- [14] C. Lin, J. D. Protasiewicz, E. T. Smith, T. Ren, *J. Chem. Soc., Chem. Commun.* **1995**, 2257–2258.
- [15] C. Lin, J. D. Protasiewicz, E. T. Smith, T. Ren, *Inorg. Chem.* **1996**, *35*, 6422–6428.
- [16] F. A. Cotton, T. Inglis, M. Kilner, T. R. Webb, *Inorg. Chem.* **1975**, *14*, 2023–2026.
- [17] F. A. Cotton, L. M. Daniels, C. A. Murillo, D. J. Timmons, *Chem. Commun.* **1997**, 1449–1450.
- [18] F. A. Cotton, X. Feng, M. Matusz, *Inorg. Chem.* **1989**, *28*, 594–601.
- [19] F. A. Cotton, S. C. Haefner, A. P. Sattelberger, *Inorg. Chem.* **1996**, *35*, 7350–7357.
- [20] F. A. Cotton, W. H. Ilsley, W. Kaim, *Inorg. Chem.* **1980**, *19*, 2360–2364.
- [21] F. A. Cotton, T. Ren, *J. Am. Chem. Soc.* **1992**, *114*, 2495–2502.
- [22] F. A. Cotton, L. M. Daniels, J. H. Matonic, C. A. Murillo, *Inorg. Chim. Acta* **1997**, *256*, 277–282.
- [23] F. A. Cotton, L. M. Daniels, L. R. Falvello, J. H. Matonic, C. A. Murillo, *Inorg. Chim. Acta* **1997**, *256*, 269–275.
- [24] F. A. Cotton, L. M. Daniels, C. A. Murillo, *Inorg. Chim. Acta* **1994**, *224*, 5–9.
- [25] F. A. Cotton, X. Feng, C. A. Murillo, *Inorg. Chim. Acta* **1997**, *256*, 303–308.
- [26] C. Lin, T. Ren, E. J. Valente, J. D. Zubkowski, E. T. Smith, *Chem. Lett.* **1997**, 753–754.
- [27] C. Lin, T. Ren, E. J. Valente, J. D. Zubkowski, *J. Chem. Soc., Dalton Trans.* **1998**, 571–576.
- [28] C. Lin, T. Ren, E. J. Valente, J. D. Zubkowski, *J. Organomet. Chem.* **1999**, *579*, 114–121.
- [29] F. A. Cotton, T. Ren, *Inorg. Chem.* **1991**, *30*, 3675–3679.
- [30] J. Bear, B. Han, S. Huang, K. Kadish, *Inorg. Chem.* **1996**, *35*, 3012–3021.
- [31] F. A. Cotton, T. Ren, *Inorg. Chem.* **1995**, *34*, 3190–3193.
- [32] Y. Li, B. Han, K. Kadish, J. L. Bear, *Inorg. Chem.* **1993**, *32*, 4175–4176.
- [33] F. A. Cotton, T. Ren, J. L. Eglin, *Inorg. Chem.* **1991**, *30*, 2559–2563.
- [34] L. P. He, C. L. Yao, M. Naris, J. C. Lee, J. D. Korp, J. L. Bear, *Inorg. Chem.* **1992**, *31*, 620–625.
- [35] F. A. Cotton, L. M. Daniels, D. J. Maloney, J. H. Matonic, C. A. Murillo, *Inorg. Chim. Acta* **1997**, *256*, 283–289.
- [36] F. A. Cotton, L. M. Daniels, X. Feng, D. J. Maloney, J. H. Matonic, C. A. Murillo, *Inorg. Chim. Acta* **1997**, *256*, 291–301.
- [37] F. A. Cotton, L. M. Daniels, D. J. Maloney, C. A. Murillo, *Inorg. Chim. Acta* **1996**, *249*, 9–11.
- [38] J. C. Le, M. Y. Chavan, L. K. Chau, J. L. Bear, K. M. Kadish, *J. Am. Chem. Soc.* **1985**, *107*, 7195–7197.
- [39] S. L. Schiavo, G. Bruno, P. Zanello, F. Laschi, P. Piraino, *Inorg. Chem.* **1997**, *36*, 1004–1012.
- [40] P. Piraino, G. Bruno, S. L. Schiavo, F. Laschi, P. Zanello, *Inorg. Chem.* **1987**, *26*, 2205–2211.
- [41] J. L. Bear, C. L. Yao, R. S. Lifsey, J. D. Korp, K. M. Kadish, *Inorg. Chem.* **1991**, *30*, 336–340.
- [42] D. I. Arnold, F. A. Cotton, D. J. Maloney, J. H. Matonic, C. A. Murillo, *Polyhedron* **1997**, *16*, 133–141.
- [43] C. Lin, J. D. Protasiewicz, T. Ren, *Inorg. Chem.* **1996**, *35*, 7455–7458.
- [44] F. A. Cotton, M. Matusz, R. Poli, X. Feng, *J. Am. Chem. Soc.* **1988**, *110*, 1144–1154.
- [45] C. L. Yao, L. P. He, J. D. Korp, J. L. Bear, *Inorg. Chem.* **1988**, *27*, 4389–4395.
- [46] F. A. Cotton, J. H. Matonic, C. A. Murillo, *Inorg. Chem.* **1996**, *35*, 498–503.
- [47] F. A. Cotton, J. H. Matonic, C. A. Murillo, *Inorg. Chim. Acta* **1997**, *264*, 61–65.
- [48] F. A. Cotton, X. Feng, M. Matusz, R. Poli, *J. Am. Chem. Soc.* **1988**, *110*, 7077–7083.

- [49] T. Ren, C. Lin, P. Amalberti, D. Macikenas, J. D. Protasiewicz, J. C. Baum, T. L. Gibson, *Inorg. Chem. Commun.* **1998**, *1*, 23–26.
- [50] Y. Zhou, D. S. Richeson, *Inorg. Chem.* **1996**, *35*, 1423–1424.
- [51] Y. Zhou, D. S. Richeson, *J. Am. Chem. Soc.* **1996**, *118*, 10850–10852.
- [52] K. M. Carlson-Day, J. L. Eglin, C. Lin, L. T. Smith, R. J. Staples, D. O. Wipf, *Polyhedron* **1999**, *18*, 817–824.
- [53] T. Ren, *Coord. Chem. Rev.* **1998**, *175*, 43–58.
- [54] P. Zuman, *The Elucidation of Organic Electrode Processes*; Academic Press, New York **1969**.
- [55] L. P. Hammett, *Physical Organic Chemistry*; McGraw-Hill, New York **1970**.
- [56] J. Shorter, *Correlation Analysis in Organic Chemistry*; Clarendon Press, Oxford **1973**.
- [57] J. E. Leffler, E. Grunwald, *Rates and Equilibria of Organic Reactions*; John Wiley and Sons, New York **1963**.
- [58] F. A. Cotton, R. A. Walton, *Multiple Bonds between Metal Atoms*, 2nd edition; Oxford University Press, Oxford **1993**.
- [59] K. M. Carlson-Day, Judith L. Eglin, L. T. Smith, R. J. Staples, *Inorg. Chem.* **1999**, *38*, 2216–2220.
- [60] L. Pauling, *The Nature of the Chemical Bond*; Cornell University Press, Ithaca, New York **1960**.
- [61] K. M. Carlson-Day, J. L. Eglin, C. Lin, T. Ren, E. J. Valente, J. D. Zubkowski, *Inorg. Chem.* **1996**, *35*, 4727–4732.
- [62] V. Srinivasan, R. A. Walton, *Inorg. Chem.* **1980**, *19*, 1635–1640.
- [63] B. E. Bursten, F. A. Cotton, A. H. Cowley, B. E. Hanson, M. Lattman, G. G. Stanley, *J. Am. Chem. Soc.* **1979**, *101*, 6244–6249.
- [64] A. J. Bard, L. R. Faulkner, *Electrochemical Methods*; John Wiley and Sons, New York **1980**.
- [65] D. H. Evans, K. Hu, *J. Chem. Soc., Faraday Trans.* **1996**, *92*, 3983–3990.
- [66] J.-F. Capon, R. Kergoat, N. L. Berre-Cosquer, S. Peron, J.-Y. Saillard, J. Talarmin, *Organometallics* **1997**, *16*, 4645–4656.
- [67] K. Hu, D. H. Evans, *J. Phys. Chem.* **1996**, *100*, 3030–3036.
- [68] G. J. Wagner, J. Q. Chambers, *Langmuir* **1997**, *13*, 3529–3541.
- [69] D. T. Pierce, W. E. Geiger, *J. Am. Chem. Soc.* **1992**, *114*, 6063–6073.
- [70] F. A. Cotton, C. A. James, *Inorg. Chem.* **1992**, *31*, 5298–5307.
- [71] T. J. Barder, R. A. Walton, *Inorg. Chem.* **1982**, *21*, 2510–2511.
- [72] F. A. Cotton, N. F. Curtis, B. F. G. Johnson, W. R. Robinson, *Inorg. Chem.* **1965**, *4*, 326–330.
- [73] W. Bradley, I. Wright, *J. Chem. Soc.* **1956**, 640–648.
- [74] Crystallographic data (excluding structure factors) for the structures reported in this paper have been deposited with the Cambridge Crystallographic Data Center as supplementary publication nos. CCDC-116605 (**1**), -116606 (**2**), -116609 (**9**), -116607 (**10a**), and -116605 (**10b**). Copies of the data may be obtained free of charge on application to CCDC, 12 Union Road, Cambridge CB2 1EZ, UK [Fax: (internat.) + 44-1223/336-033; E-mail: deposit@ccdc.cam.ac.uk].
- [75] *SMART V 4.043 Software for the CCD Detector System*, Siemens Analytical Instruments Division, Madison, WI, **1996**.
- [76] *SAINT V 4.035 Software for the CCD Detector System*, Siemens Analytical Instruments Division, Madison, WI, **1995**.
- [77] “SADABS, Program for Absorption corrections using Siemens CCD based on the method of Bob Blessing”, *Acta Crystallogr.* **1995**, *A51*, 33.
- [78] G. M. Sheldrick, *SHELXL-90, Program for the Solution of Crystal Structures*, University of Göttingen, Germany, **1986**.
- [79] G. M. Sheldrick, *SHELXL-93, Program for the Refinement of Crystal Structures*, University of Göttingen, Germany, **1993**.
- [80] *SHELXTL 5.03 (PC Version), Program Library for Structure Solution and Molecular Graphics*, Siemens Analytical Instruments Division, Madison, WI, **1995**.

Received April 6, 1999
[199116]